FACTA UNIVERSITATIS
Series: **Mechanical Engineering**
https://doi.org/10.22190/FUME201212003Z

Original scientific paper

FRACTAL APPROACH TO MECHANICAL AND ELECTRICAL PROPERTIES OF GRAPHENE/SIC COMPOSITES

Yu-Ting Zuo[1,2], Hong-Jun Liu[1,2]

[1]School of Materials Science and Engineering, Lanzhou University of Technology, China
[2]State Key Laboratory of Advanced Processing and Recycling of Non-ferrous Metals, Lanzhou University of Technology, China

Abstract. *Graphene and carbon nanotubes have a Steiner minimum tree structure, which endows them with extremely good mechanical and electronic properties. A modified Hall-Petch effect is proposed to reveal the enhanced mechanical strength of the SiC/graphene composites, and a fractal approach to its mechanical analysis is given. Fractal laws for the electrical conductivity of graphene, carbon nanotubes and graphene/SiC composites are suggested using the two-scale fractal theory. The Steiner structure is considered as a cascade of a fractal pattern. The theoretical results show that the two-scale fractal dimensions and the graphene concentration play an important role in enhancing the mechanical and electrical properties of graphene/SiC composites. This paper sheds a bright light on a new era of the graphene-based materials.*

Key Words: *Steiner Minimum Tree Structure, 3D Printing, Graphene-based Composites, Two-scale Fractal Dimension*

1. INTRODUCTION

Graphene is a two-dimensional nanomaterial with a Steiner minimum tree structure [1,2] characterized by the most stable structure and network optimization, see Fig. 1. The Steiner structure is also seen in natural phenomena, for example, multiple bubbles' interaction leads to such a structure and it is used for nanofiber fabrication by the bubble electrospinning [3,4,5]. Fig. 2 is a photograph of dry cracked soil, and it can be seen that the cracks meet the requirements of the Steiner minimum tree structure. The trusswork with the Steiner minimum tree structure has the most stable and good mechanical property.

Received December 12, 2020 / Accepted January 05, 2020
Corresponding author: Yu-Ting Zuo
Lanzhou University of Technology, Lanzhou 730050, China
E-mail: zuoyuting2020@126.com

Likewise, graphene also has very stable chemical and mechanical properties. The network optimization characteristics of graphene give it excellent thermal and electrical conductivity properties; as a result high electronic and thermal conductivities are predicted.

Graphene/SiC composites are widely used in various fields, from ceramics to building materials, and the three-dimensional printing technology is now available for advanced fabrication of graphene/SiC composites [6-9].

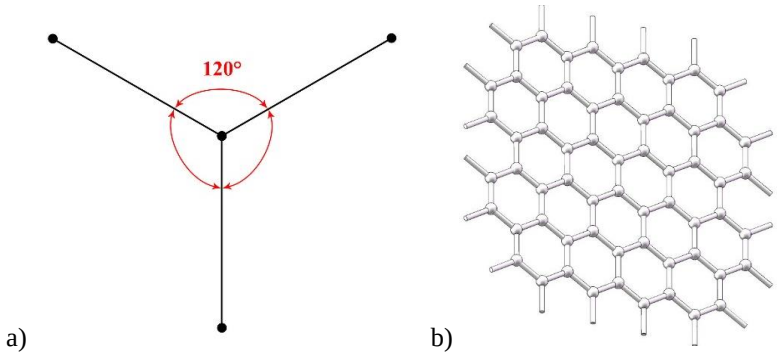

Fig. 1 (a) Steiner minimum tree structure and (b) Steiner minimum tree structure in graphene

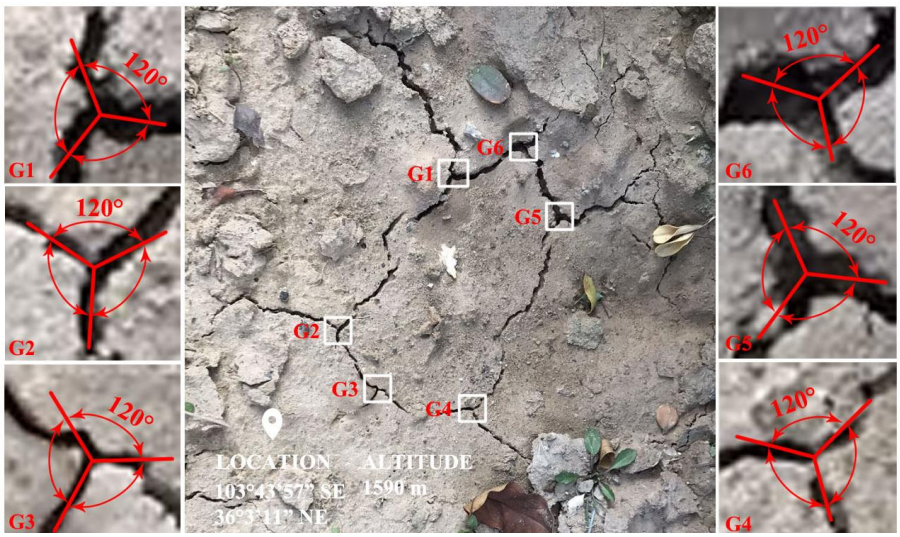

Fig. 2 Cracked land with minimal tree structure

Graphene is the hardest material found so far, and has an excellent mechanical property as well; it is one of the materials with the highest known strength. At the same time, it has good toughness and can be bent with ease. The specific surface area of graphene is up to 2600m^2/g. In addition, graphene has good electrical conductivity; at room temperature, its electron mobility can be as high as 20000cm^2/(V·s), which is more than 10 times that of silicon and more than twice that of indium antimonide (InSb).

Table 1 compares the mechanical, thermodynamic and electrical properties of graphene with other materials. Due to its unique properties, graphene is widely used to enhance the mechanical and electronic properties of various functional composites.

Table 1 Properties of graphene, CNT, nano-sized steel and polymers [10]

Materials	Tensile strength	Thermal conductivity at room temperature (W/mK)	Electronic conductivity(S/m)
graphene	130±10GPa	(4.84±0.44)×103 to (5.30±0.48)×103	7200
CNT	60~150GPa	3500	3000~4000
nano-sized steel	1769MPa	5~6	1.35×106
HDPE plastic	18~20MPa	0.46~0.52	Insulator
Natural rubber	20~30	0.13~0.142	Insulator
Kevlar fiber	3620MPa	0.04	Insulator

2. Mechanical Property

A smaller grain size results in a stronger material; this can be explained by the well-known Hall-Petch effect [11,12], which is widely used in material design, that is, adding nano or micro particles can improve the mechanical properties of materials. In 1951, Hall found the relationship between crystal particle size and yield strength. In 1953, Petch discovered that crystal size also had a similar relationship with brittle fracture. The Hall -Petch effect was described in a mathematical expression [11,12]:

$$\sigma = \sigma_0 + \frac{k}{d^{\beta}} \tag{1}$$

Here, σ is the elastic modulus or strength, σ_0 is the parent property of the material, k is the material constant, d is the average diameter of the particle, β is the geometric constant, and it is related to the volume percentage of the additive.

The Hall-Petch effect cannot describe the effects of the size distribution surface morphology of particles on the mechanical property; additionally, when the particles tend to be small enough, an inverse Hall-Petch effect occurs [11], so a modified Hall-Petch effect is much needed to take into account the particles' surface morphology. For graphene-reinforced composites, see Fig.3, considering the two-dimensional characteristics of graphene, d, can be obtained by using the equivalent diameter:

$$d = (\frac{6\delta A}{\pi})^{1/3} \tag{2}$$

where A is the average area of graphene and δ is the thickness of graphene.

We obtain the following modified Hall-Petch effect formula

$$\sigma = \sigma_0 + \frac{k'}{A^{\beta/3}} \tag{3}$$

where k' is the material constant.

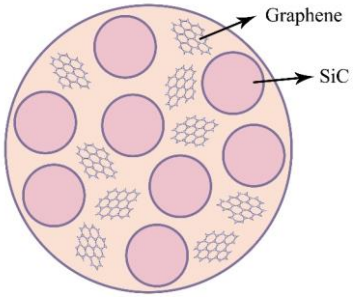

Fig. 3 Microstructure of graphene composites

The mechanical properties of composites can be enhanced by adding graphene, which can be qualitatively described by the Hall-Petch effect. For isotropic elastic materials, the stress formula is

$$\sigma = \frac{F}{A} \tag{4}$$

Here σ is the stress, F is the external force applied, and A is the area of the cross section of the object.

Fig. 4(a) is a force analysis diagram of a control body containing graphene. The control body is fractured under external forces, and the fracture surface is unsmooth as shown in Fig. 4(b).

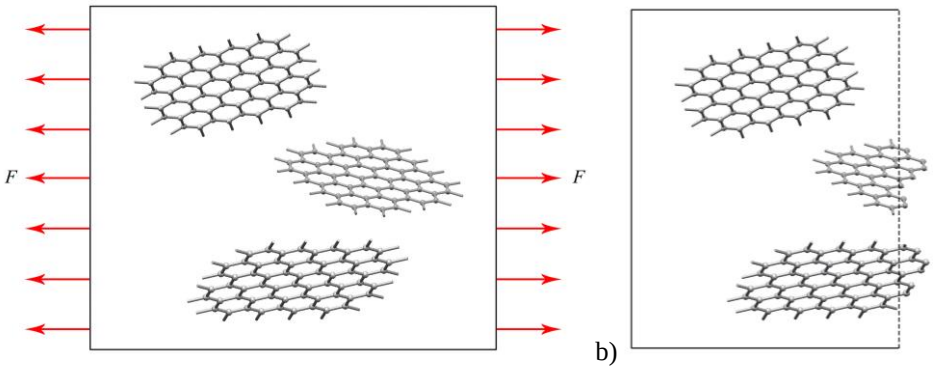

Fig. 4 Force analysis of the composite control body containing graphene

The control body in Fig. 4(a) can be divided into two parts, SiC matrix and graphene. Before breaking, the matrix needs to overcome the friction resistance between the matrix and the graphene, which is very high due to an extremely large specific surface area of the graphene. In addition, the fracture surface contains a lot of graphene, which is not smooth. To sum up, the force balance equation can be written

$$F = \sigma A + f \tag{5}$$

where F is the external force, F is the frictional resistance between the matrix and the graphene, and A is the area of the non-smooth section, which can be expressed as:

$$A = A_0 + \Delta A \tag{6}$$

where A_0 is the smooth cross section area, ΔA is proportional to the specific surface parameters of graphene.

The real stress of the matrix of the composite material is

$$\sigma = \frac{F - f}{A_0 + \Delta A} \tag{7}$$

The frictional resistance between the matrix and the graphene is proportional to the surface area of graphene; if the percentage of the volume of graphene is φ, we have

$$f \propto S \propto \varphi^{2/3} \tag{8}$$

$$\Delta A \propto S \propto \varphi^{2/3} \tag{9}$$

where φ is the volume concentration.

Eq. (7) becomes

$$\sigma = \frac{F - a\varphi^{2/3}}{A + b\varphi^{2/3}} = \frac{\sigma_0 - \tilde{a}\varphi^{2/3}}{1 + \tilde{b}\varphi^{2/3}} \tag{10}$$

where a and b are constants, $\sigma_0 = F / A$, $\tilde{a} = a / A$ and $\tilde{b} = b / A$. Fig. 5 shows the effect of graphene content on the stress of the composites under the same force.

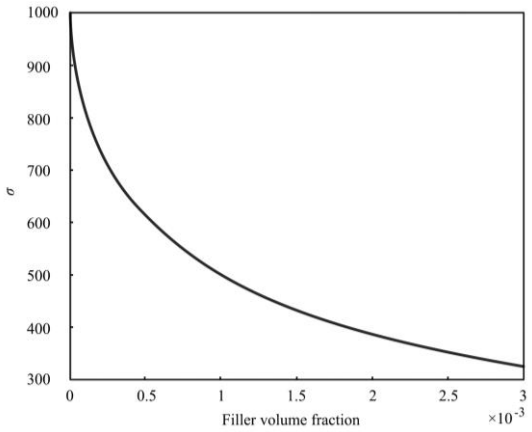

Fig. 5 The effect of the graphene content on the stress of the composites under the same force ($\tilde{a} = \tilde{b}$=100, σ_0=1000)

To obtain a formula similar to the Hall-Petch effect, we make a simple mathematical approximation to formula (10). Let

$$x = \varphi^{2/3} \tag{11}$$

Eq. (10) becomes

$$\sigma(x)=\frac{F-ax}{A+bx} \tag{12}$$

Differentiating Eq. (12) with respect to x, we have

$$\sigma'(x)=\frac{-a(A+bx)-b(F-ax)}{(A+bx)^2} \tag{13}$$

Setting x=0, we have

$$\sigma(0)=\frac{F}{A} \tag{14}$$

$$\sigma'(0)=\frac{-aA-bF}{A^2} \tag{15}$$

Its first order Taylor series approximation is

$$\sigma(x)=\sigma(0)+\sigma'(0)x=\sigma_0+\frac{aA+bF}{A^2}x \tag{16}$$

That is

$$\sigma=\sigma_0+k\varphi^{2/3} \tag{17}$$

So we obtain the following formulation similar to the Hall-Petch effect

$$\sigma=\sigma_0-k+\frac{k}{1-\varphi^{2/3}} \tag{18}$$

where $k=\frac{aA+bF}{A^2}$. Table 2 shows the effect of the graphene content on the fracture strength of PVA/ graphene composites [10].

Table 2 Influence of the graphene content on the fracture strength of PVA/ graphene composites [10]

φ (%)	0	0.3	0.5	0.7
σ_0(MPa)	49.7	68.2	72.2	87.8

According to the data in Table 2, we can approximately determine that k=13.2165, so that

$$\sigma=\sigma_0-13.2165+\frac{13.2165}{1-\varphi^{2/3}} \tag{19}$$

Fig. 6 shows the stress-strain behavior for PVA/graphene nanocomposites with different GO weight loadings. With only 0.7 wt.% GO, the tensile strength of the nanocomposite increased by 76% from 49.9 to 87.6 MPa [10].

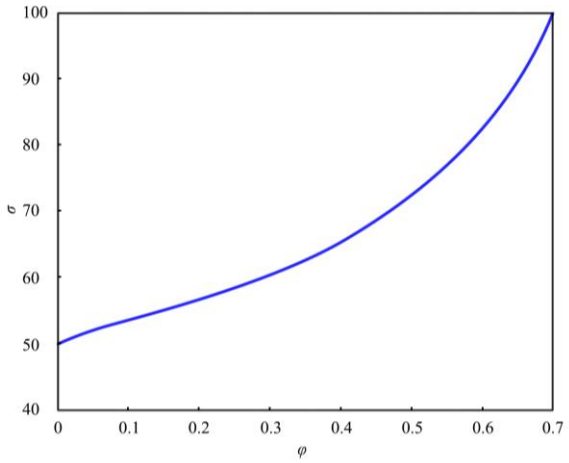

Fig. 6 Stress-strain behavior for PVA/graphene nanocomposites with different GO weight loadings. With only 0.7 wt.% GO, the tensile strength of the nanocomposite increased by 76% from 49.9 to 87.6 MPa [10]

3. Electronic Property

According to Ohm's formulation, the resistance of a metal rod can be expressed as

$$R = \frac{kL}{S} \tag{20}$$

where R, L, and S represent, respectively, the resistance, the length and the area of the conductor, k is a constant.

However, for a carbon nanotube, the resistance can be expressed as [13]

$$R \propto L^{\alpha} \tag{21}$$

where α is the fractal dimensions of the carbon nanotube, and it can be calculated as α=2.52 [13].

The fractal theory has become a useful tool to various engineering problems, for examples, non-smooth fibers [14], the fractal current law [15], the fractal pressure drop through a cigarette filter[16], fractal-like multiple jets in electrospinning process [17], the fractional Fokker-Planck equation [18], the fractional Kundu–Mukherjee–Naskar equation [19], the fractal Telegraph equation[20], and fractal integral equations and fractal oscillators [21,22], the fractal Boussinesq equation [23], the fractal microgravity [24],the fractal Bratu-type equation [25], the fractal diffusion [26], the fractal two-phase flow [27], the fractal boundary problems [28], and the fractal convection-diffusion law [29].

In this paper we will apply the fractal theory to the study of the electronic properties of carbon nanotubes [30,31], graphene and graphene-based composites.

The fractal dimension can be calculated as

$$\alpha = \frac{\ln M}{\ln N} \tag{22}$$

where M is the new number of the measured units under a reduced size of $1/N$. For example, the fractal dimensions for the Koch curve is ln4/ln3, while the Cantor set is ln2/ln3, and the Sierpinski triangle is ln3/ln2.

In Ref. [13], the graphene or the carbon nanotube is considered as a graphene fractal as illustrated in Fig. 7.

The fractal dimension of the graphene fractal is

$$\alpha = \frac{\ln 5}{\ln 4} = 1.16096 \tag{23}$$

Eq. (23) describes exactly a fractal pattern as illustrated in Fig. 7, the initial iteration is a graphene unit, and the iteration process can continue to infinity. The value of the fractal dimensions is an important factor to describe the self-similarity of a geometric patterner. However, for a practical application, a discontinuous geometric patterner can be considered as some cascade of a self-similar fractal one. For example, we have two adjacent cascades of the Sierpinski triangle, see Fig. 8. Their porosity factors are quite different, and we need the two-scale fractal dimensions to measure the difference [32-35].

The two-scale fractal theory has been widely used as an effective mathematics tool to analyze various discontinuous problems, for examples, fractional Camassa-Holm equation [36], biomechanism of silkworm cocoon[37], snow's thermal insulation [38], fractal calculus for analysis of wool fiber [39] and polar bear hairs [40,41].

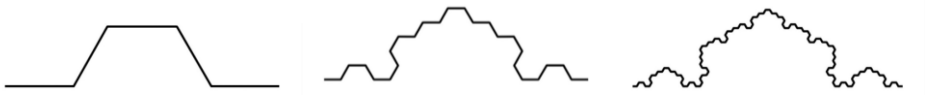

Fig. 7 The graphene fractal

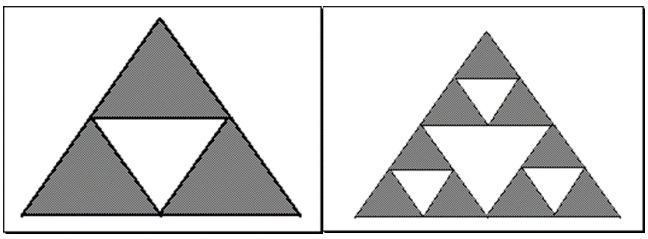

Fig. 8 Two adjacent levels of the Sierpinski triangle with fractal dimensions of ln3/ln2.

The two-scale fractal dimension is defined as [32-35]

$$\alpha = \alpha_0 \times \frac{L}{L_0} \tag{24}$$

where α and α_0 are dimensions for the two scales, respectively, one is large and the other is smaller; L and L_0 are, respectively, the measured units (e.g. length, area or volume) for the two scales. For the two adjacent levels of the Sierpinski triangle given in Fig. 8, the two-scale fractal dimensions are 3/2 and 9/8, respectively.

Consider a unit of the graphene as illustrated in Fig. 9; we have L/L_0=5/4 and α_0=2, and

$$\alpha = 2 \times \frac{5}{4} = 2.5 \tag{25}$$

According to Eq. (21), the resistance of a carbon nanotube can be expressed as

$$R = kL^{2.5} \tag{26}$$

Using the experimental data given in Ref. [42], we can identify the value of k in Eq. (26), and obtain the following relationship

$$R = 94.5L^{2.5} \tag{27}$$

This is quite close to R=95$L^{2.52}$, which was given in Ref. [13]. Comparison of our theoretical result given by Eq. (27) with the experimental data from Ref. [42] is depicted in Fig.10.

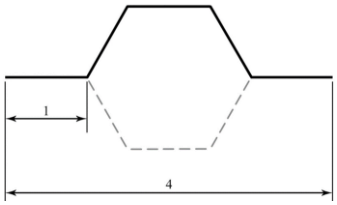

Fig. 9 A unit of the two-dimensional graphene

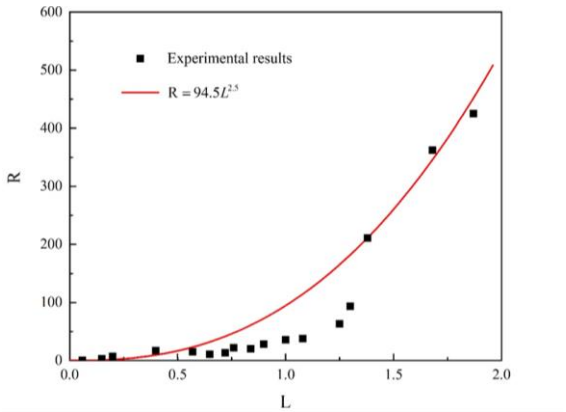

Fig. 10 Resistance (kΩ) versus length (μm) for SWNTs. The dots are experimental data [42], the continuous line is the theoretical prediction according to the two-scale fractal theory

Graphene/SiC composites are widely used in engineering, especially advanced materials science and smart ceramics, and their electrical property is the focus for various applications.

Consider a rod of graphene/SiC composite as illustrated in Fig. 11. Graphene-based composite materials have attracted much attention due to their extremely good thermal and electronic properties [10,42].

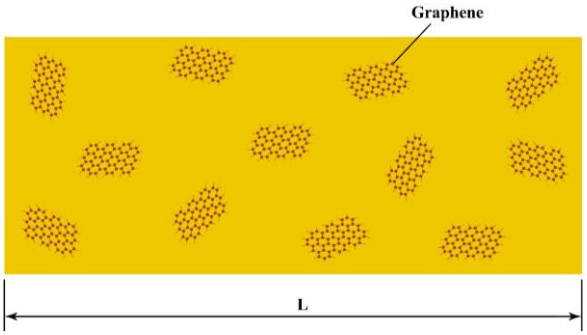

Fig. 11 Graphene/SiC composite

Electrical conductivity of continuous non-metal materials scales with its length with a negative power

$$C \propto L^{-\alpha} \tag{28}$$

We already know that the addition of graphene can greatly enhance the electrical conductivity of the composite. The equivalent length of graphene and the equivalent length of SiC material can be expressed as

$$L_{Graphene} \propto \left(\frac{V_{Graphene}}{\delta} \right)^{1/2} \tag{29}$$

$$L_{SiC} \propto (V_{SiC})^{1/3} \tag{30}$$

where $L_{Graphene}$ is the equivalent length of graphene, δ is the thickness of the graphene, L_{SiC} is the equivalent length of SiC material, $V_{Graphene}$ and V_{SiC} are, respectively, the total volumes of graphene and SiC in the composite.

We assume that the graphene concentration in the composite is φ, which implies

$$V_{Graphene} = V_0 \varphi \tag{31}$$

$$V_{SiC} = V_0 (1-\varphi) \tag{32}$$

where V_0 is the total volume of the composite.

After a simple operation, we have the following scaling laws

$$L_{Graphene} \propto \varphi^{1/2} \tag{33}$$

$$L_{SiC} \propto (1-\varphi)^{1/3} \tag{34}$$

The electrical conductivity of graphene and the resistance of SiC are, respectively, as follows

$$C_{Graphene} \propto \varphi^{\alpha_1/2} \tag{35}$$

$$C_{SiC} \propto (1-\varphi)^{\alpha_2/3} \tag{36}$$

where α_1 and α_2 are two-scale dimensions for graphene and SiC material, respectively. According to the analysis given in the above section, we have α_1=2.5, which implies

$$C_{Graphene} \propto \varphi^{1.25} \tag{37}$$

The total resistance of the graphene/SiC composite can be expressed as

$$R = R_{Graphene} + R_{SiC} = k_1\varphi^{-1.25} + k_2(1-\varphi)^{\alpha_2/3} \tag{38}$$

where k_1 and k_2 are constants in this study.

Electrical conductivity of graphene/SiC composites can be expressed as

$$C = \frac{1}{k_1\varphi^{-1.25} + k_2(1-\varphi)^{\alpha_2/3}} \tag{39}$$

where k_1 and k_2 are constants in this study. In most cases, $k_1 >> k_2$, and Eq. (39) can be approximated as

$$C = C_0 + k\varphi^{1.25} \tag{40}$$

In Ref. [42] three powder compositions were prepared with increasing GNPs contents, specifically 5, 10 and 20 vol.% were used to measure the electrical conductivity of the graphene/SiC composite. The results are listed in Table 3.

Table 3 Electrical conductivity of the graphene/SiC composite with different GNPs contents [42]

φ (%)	0	0.05	0.10	0.20
C(S/m)	17	305	933	2306
Porosity(%)	0.5	0.6	0.65	0.70
α_2	1.5	1.8	1.95	2.1

According to the above experimental data, we know C_0=17 S/m, and constant k involved in Eq. (40) can be approximately determined; finally, the following equation is obtained

$$C = 17 + 15195\varphi^{1.25} \tag{41}$$

Fig. 12 shows the comparison between our theoretical prediction and the experimental data, and a good agreement is obtained.

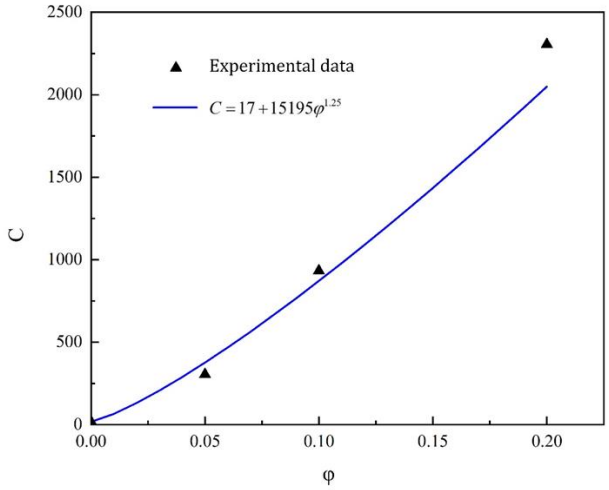

Fig. 12 The electrical conductivity of the graphene/SiC composite rod

4. Discussion and Conclusion

Many experiments have proved that an increase of GO concentration will enhance the SiC/graphene composite's mechanical property; however, similarly to the inverse Hall-Petch effect, when the concentration of GO increases to a threshold value, an inverse effect can be predicted.

Recently Le et al. suggested a theoretical method for graphene-reinforced composites, showing a bright light on the optimal design of SiC/ graphene composites for advanced applications [43].

This paper suggests, for the first time, some new concepts for graphene/SiC composites, e.g., the graphene fractal and the two-scale porosity. A fractal modification of Ohm's resistance formulation is suggested, and our theoretical prediction sees a good agreement with the experiment results given in Ref. [40]. Furthermore, the mechanical and electrical properties of the graphene/SiC composites are theoretically analyzed by the two-fractal theory and experimentally verified by open experimental data in literature [10, 42].

Acknowledgements*: The authors wish to acknowledge the financial support for this work from the School of Materials Science and Engineering of Lanzhou University of Technology, and wish to thank teachers from the State Key Laboratory of Advanced Processing and Recycling of Non-ferrous Metals for technical support.*

References

1. Novoselov, K.S., Geim, A.K., Morozov, S.V., Jiang, D., Zhang, Y., Dubonos, S.V., Grigorieva, I.V., Firsov, A.A., 2004, *Electric field effect in atomically thin carbon films*, Science, 306(5696), pp. 666-669.
2. Geim, A.K., Novoselov, K.S., 2007, *The rise of graphene*, Nature Materials, 6(2007), pp. 183-191.
3. Li, X.-X., Xu, L.-Y., He, J.-H., 2020, *Nanofibers membrane for detecting heavy metal ions*, Thermal Science, 24(4), pp. 2463-2468.

4. Yao, X., He, J.-H.,2020, *On fabrication of nanoscale non-smooth fibers with high geometric potential and nanoparticle's non-linear vibration*, Thermal Science, 24(4), pp. 2491-249.
5. Yin, J., Wang, Y., Xu, L., 2020, *Numerical approach to high-throughput of nanofibers by a modified bubble-electrospinning*, Thermal Science, 2020 24(4), pp. 2367-2375.
6. You, X., Yang, J.S., Huang, K., Wang M.M., Zhang, X.Y., Dong, S.M., 2019, *Multifunctional silicon carbide matrix composites optimized by three-dimensional graphene scaffolds*, Carbon, 155, pp. 215-222.
7. Zuo, Y.T., Liu, H.J., 2021, *A fractal rheological model for sic paste using a fractal derivative*, Journal of Applied and Computational Mechanics, 7, pp. 13-18.
8. Wang, Y.C., Zhu, Y.B., He, Z.Z., Wu, H.A., 2020, *Multiscale investigations into the fracture toughness of SiC/graphene composites: Atomistic simulations and crack-bridging model*, Ceramics International , 46(18A), pp. 29101-29110.
9. Gnatowski, A., Kijo-Kleczkowska, A., Otwinowski, H., Sikora, P., 2019, *The research of the thermal and mechanical properties of materials produced by 3D printing method*, Thermal science, 23(Suppl. 4), pp. 1211-1216.
10. Kuilla, T., Bhadra, S., Yao, D., Kim, N.H., Bose, S., Lee, J.H., 2010, Recent advances in graphene based polymer composites, Progress in Polymer Science, 35(11), pp. 1350-1375.
11. Tian, D., Zhou, C.J., He, J.H., 2018, *Hall-Petch effect and inverse Hall-Petch effect: A fractal unification*, Fractals, 6(26), 1850083.
12. Tian, D., Zhou, C.J., He, J.H., 2019, *Strength of bubble walls and the Hall–Petch effect in bubble-spinning*, Textile Research Journal, 89(7), pp. 1340-1344.
13. He, J.H., 2008, *A new resistance formulation for carbon nanotubes*, Journal of Nanomaterials, doi: 10.1155/2008/954874.
14. Yao, X., He, J.H., 2020, *On fabrication of nanoscale non-smooth fibers with high geometric potential and nanoparticle's non-linear vibration*, Thermal Science, 24(4), pp. 2491-2497.
15. Xu, L.Y., Li, Y., Li, X.X., He, J.H., 2020, *Detection of cigarette smoke using a fiber membrane filmed with carbon nanoparticles and a fractal current law*, Thermal Science, 24(4), pp. 2469-2474.
16. Yang, Z.P., Li, Z., Feng, D., Li, J., Feng, X.M., 2020, *A fractal model for pressure drop through a cigarette filter*, Thermal Science, 24(4), pp. 2653-2659.
17. Wu, Y.K., Liu, Y.,2020, *Fractal-like multiple jets in electrospinning process*, Thermal Science, 24(4), pp. 2499-2505.
18. Deng, S.X., Ge, X.X., 2020, *Fractional Fokker-Planck equation in a fractal medium*, Thermal Science, 24(4), pp. 2589-2595.
19. He, J.H., El-Dib, Y.O., 2020, *Periodic property of the time-fractional Kundu-Mukherjee-Naskar equation*, Results in Physics, 19, 103345.
20. He, J.H., 2020, *On the fractal variational principle for the telegraph equation*, Fractals, doi: 10.1142/S0218348X21500225.
21. He, J.H., 2020, *A simple approach to Volterra-Fredholm integral equations*, Journal of Applied and Computational Mechanics, 6(SI), pp. 1184-1186.
22. He, J.H., 2019, *The simpler, the better: Analytical methods for nonlinear oscillators and fractional oscillators*, Journal of Low Frequency Noise Vibration and Active Control, 38(3-4), pp. 1252-1260.
23. Ji, F.Y., He, C.H., Zhang, J.J., He, J.H., 2020, *A fractal Boussinesq equation for nonlinear transverse vibration of a nanofiber-reinforced concrete pillar*, Applied Mathematical Modelling, 82, pp. 437-448.
24. He, J.H., 2020, *A fractal variational theory for one-dimensional compressible flow in a microgravity space*, Fractals, 28(02), 2050024.
25. He, C.H., Shen, Y., Ji, F.Y., He, J.H., 2020, *Taylor series solution for fractal Bratu-type equation arising in electrospinning process*, Fractals, 28(01), 2050011.
26. Lin, L., Yao, S.W., 2019, *Fractal diffusion of silver ions in hollow cylinders with unsmooth inner surface*, Journal of Engineered Fibers and Fabrics, 14(1), 1558925019895643.
27. Li, X., Liu, Z., He, J.H., 2020, *A fractal two-phase flow model for the fiber motion in a polymer filling process*, Fractals, 28(5), 2050093.
28. He, J.H., 2020, *A short review on analytical methods for a fully fourth-order nonlinear integral boundary value problem with fractal derivatives*, International Journal of Numerical Methods for Heat and Fluid Flow, doi: 10.1108/HFF-01-2020-0060.
29. He, J.H., 2019, *A simple approach to one-dimensional convection-diffusion equation and its fractional modification for E reaction arising in rotating disk electrodes*, Journal of Electroanalytical Chemistry, 854, 113565.

30. Randjbaran, E., Majid, D.L., Zahari, R., Sultan, M.T.B.H., Mazlan, N., 2020, *Effects of volume of carbon nanotubes on the angled ballistic impact for carbon kevlar hybrid fabrics*, Facta Universitatis-Series Mechanical Engineering, 18(2), pp. 1-16.
31. Rysaeva, L.K., Korznikova, E.A., Murzaev, R.T., Abdullina, D.U., Kudreyko, A., Baimova, Y.A., Lisovenko, D., Dmitriev, Sergey V., 2020, *Elastic damper based on the carbon nanotube bundle*, Facta Universitatis-Series Mechanical Engineering, 18(1), pp. 1-12.
32. He, J.H., Ain, Q.T., 2020, *New promises and future challenges of fractal calculus: from two-scale thermodynamics to fractal variational principle*, Thermal Science, 24(2A), pp. 659-681.
33. Ain, Q.T., He, J.H, 2019, *On two-scale dimension and its applications*, Thermal Science, 23(3), pp. 1707-1712.
34. He, J.H., 2018, *Fractal calculus and its geometrical explanation*, Results in Physics, 10, pp. 272-276.
35. He, J.H., 2020, *Thermal science for the real world: Reality and challenge*, Thermal Science, 24(4), pp.2289-2294.
36. Anjum, N., Ain, Q.T., 2020, *Application of he's fractional derivative and fractional complex transform for time fractional camassa-holm equation*, Thermal Science, 24(5), pp. 3023-3030.
37. Liu, F.J., Zhang, X.J., Li, X., 2019, *Silkworm (bombyx mori) cocoon vs. wild cocoon multi-layer structure and performance characterization*, Thermal Science, 23(4), pp. 2135-2142.
38. Wang, Y., Yao, S.W., Yang, H.W., 2019, *A fractal derivative model for snow's thermal insulation property*, Thermal Science, 23(4), pp. 2351-2354.
39. Fan, J., Yang, X., Liu, Y., 2019, *Fractal calculus for analysis of wool fiber: Mathematical insight of its biomechanism*, Journal of Engineered Fibers and Fabrics, 14, doi: 10.1177/1558925019872200.
40. Wang, Q.L., Shi, X.Y., He, J.H., Li, Z.B., 2018, *Fractal calculus and its application to explanation of biomechanism of polar bear's hairs*, Fractals, 26(6), 1850086.
41. Wang, Q.L., Shi, X.Y., He, J.H., Li, Z.B., 2018, *Fractal calculus and its application to explanation of biomechanism of polar bear's hairs*, Fractals, 27(5), 1992001.
42. Sundqvist, P., Garcia-Vidal, F.J., Flores, F., Moreno-Moreno, M., Julio Gómez-Herrero, 2007, *Voltage and length-dependent phase diagram of the electronic transport in carbon nanotubes*, Nano Letters, 7(9), pp. 2568-2573.
43. Le, N.Y., Nguyen, T.P., Vu, H.N., Nguyen, T.T., Vu, M.D., 2020, *An analytical approach of nonlinear thermo-mechanical buckling of functionally graded graphene-reinforced composite laminated cylindrical shells under compressive axial load surrounded by elastic foundation*, Journal of Applied and Computational Mechanics, 6(2), pp. 357-372.